Analysis of Massive IoT Networks in Nearest and Macro Diversity Reception Regime

Tijana Devaja, Milica Petkovic, Dejan Vukobratovic
Faculty of Technical Sciences
University of Novi Sad
Novi Sad, Serbia
tijana.devaja, milica.petkovic, dejanv@uns.ac.rs

Marko Beko
Instituto de Telecomunicações, Copelabs
Instituto Superior Técnico, Universidade Lusofona
Lisbon, Portugal
beko.marko@gmail.com

***Abstract*—In this overview paper, we present a reliability analysis for massive Internet of Things (IoT) connectivity in cellular networks. In such networks, IoT devices intermittently and unpredictably transmit short data packets to base stations (BSs), often causing interference with other devices sharing the same uplink channel. Assuming a slotted ALOHA random access scheme under Nakagami fading, we investigate the probability that a short-packet transmission from an IoT device fails to be decoded, in the nearest BS and macro diversity reception regime. Using a combination of finite block-length (FBL) information theory and stochastic geometry, we derive error probability expressions. These FBL-based results are compared with existing asymptotic expressions, which assume the transmission of asymptotically long packets. Numerical results confirm the accuracy of the derived expressions and their relevance to the design and performance evaluation of massive IoT systems across a wide range of parameters.**

***Index Terms*—Stochastic geometry, short-packet communication, slotted ALOHA, Finite Block-Length.**

I. Introduction

Massive Internet of Things (IoT) cellular networks, such as Narrowband IoT (NB-IoT), LoRaWAN, and SigFox, are designed to connect billions of IoT devices that were previously beyond the reach of traditional wireless technologies [1]. A large number of deployed devices can rapidly congest the radio access network, resulting in high collision and retransmission rates, as well as reduced energy efficiency. Since these devices typically lack an external power supply, efficiently managing a vast number of devices is a critical concern for mobile network operators. In these networks, each device transmits short-packet uplinks with unpredictable activity patterns. To handle this sporadic traffic, variations of Slotted ALOHA (SA) are often used for random access [2].

However, when a device transmits in an SA-based IoT network, its signal is subject to channel impairments and interference from other active devices, while adhering to the fundamental limits of short-packet transmission, as defined by finite block-length (FBL) information theory [3]. The analysis of error probability in these short-packet IoT communications relies on two key methods: stochastic geometry for interference analysis in large-scale systems error probability assessment [4]–[6], and FBL information theory [7], [8].

In traditional cellular network analysis, stochastic geometry is widely used to study coverage probabilities in uplink and downlink transmissions [9]. These studies generally assume that a device will be successfully decoded at a base station (BS) if its signal-to-interference-and-noise ratio (SINR) exceeds a certain threshold. However, in practice, the relationship between error probability and SINR is not a sharp transition unless the system operates at the Shannon limit using asymptotically long capacity-achieving codes. For short-packet communications, the error probability vs. SINR relationship is smoother, making traditional coverage probability models only approximations of real-world performance, especially for IoT networks dominated by short packets [10].

For massive IoT networks, extending traditional analysis using FBL provides more accurate error probability estimates. The need to rethink wireless network design for short-packet communications was first discussed in [4], and while some recent works have extended these analyses to the FBL regime, they tend to focus on rate and capacity rather than reliability or explicit error probability expressions [11], [12]. In this overview paper, we review expand on our recent results in [13], [14], addressing the above mentioned gaps by improving error probability analysis for short-packet communications in massive IoT networks. First, we show how one can refine the existing threshold-based error probability results by accounting for the short-packet nature of transmissions, using FBL theory to derive new, approximate but accurate error probability expressions [14]. We present exact closed-form error probability expressions under Nakagami fading, improving upon existing results in the literature. Additionally, we compare results for error probability analysis of LP WAN Networks in nearest BS and macro diversity reception regimes [10].

The main contributions of our research [14] include the development of a approximate analysis of error probability in massive IoT networks within the FBL regime using the more general Nakagami fading model, offering broader applicability. The use of distinct analytical methods allows us to derive closed-form expressions for the probability density function (PDF) of interference, setting this study apart from previous research, which often focuses on average rate and capacity rather than explicit error probability expressions. Lastly, the analysis covers both the nearest BS case review from [13], [14] and the novel extension of previous work, macro diversity reception case, offering a comprehensive comparison.

Fig. 1. System model.

The rest of the paper is structured as follows. In Section II, we define the system model and set the main hypothesis. In Section III and IV, we analyze the error probability and channel coding rate based on the FBL regime approach for nearest BS and macro diversity reception regime, respectively. In Section V, we present and discuss the numerical results and, finally, in Section VI, we close the paper with the main conclusions.

II. System and Interference Model

We consider a large-scale wireless network comprising a set of BSs distributed according to a stationary Poisson point process (PPP) Φ_b with spatial density λ_b over the plane $\mathbb{R}^2$. The network also contains a set of user devices whose locations follow another stationary PPP Φ_u with spatial density λ_u. Devices transmit data to BSs using the SA protocol, assuming that time is divided into equal-length slots. In each slot, every device is active with probability p, independently of the activity of other devices. All active devices connect to either the geographically nearest BS or a macro BS [10]. The primary focus is on determining the probability of successful decoding for an active device at its nearest or macro BS. Stochastic geometry will be employed to analyze the aggregate interference in this large-scale network, providing insights into error probability. Assuming normalized unit transmit power and fading environment, the received power P at a reference BS at the distance r from a reference device is defined as

$$P = hr^{-\eta}, \tag{1}$$

where $r^{-\eta}$ represents path-loss attenuation with a path loss exponent η, and h is the fading power channel coefficient being an exponentially distributed random variable with unit mean as shown in Fig.1.

Aggregate interference I at any given point in the network originating from the set of all transmitters is defined as

$$I = \sum_{i\in\Phi_u} P_i = \sum_{i\in\Phi_u} h_i {r_i}^{-\eta}, \tag{2}$$

where r_i is a distance of the device $i \in \Phi_u$ from the reception point, and h_i is a realization of its fading gain. Instantaneous SINR [15] of a device at the distance r from a reference BS is

$$\gamma = \frac{hr^{-\eta}}{I+\sigma^2} \approx \frac{hr^{-\eta}}{I}, \tag{3}$$

where σ^2 is the background noise power, which is usually negligible compared to the cumulative interference.

1) The PDF of the fading power: We consider Nakagami fading where the fading power H follows

$$f_H(h) = \frac{m^m}{\Gamma(m)} h^{m-1}\exp(-mh), \quad h\in(0,+\infty], \tag{4}$$

and m is the fading parameter. For $m = 1$, we obtain a special case of Rayleigh fading.

2) The PDF of the interference power: In order to determine the closed-form expression of the PDF of aggregate interference I, its Laplace transform (LT) is defined as [4]

$$\mathcal{L}_I(s) = \exp\Big(-p\lambda_u\pi\mathbb{E}\big[h^{\frac{2}{\eta}}\big]\Gamma(1-\frac{2}{\eta})s^{\frac{2}{\eta}}\Big), \tag{5}$$

where $\Gamma(z)$ is the Gamma function [16, (8.31)] and $\mathbb{E}[\cdot]$ is the expectation operator. For gamma distributed fading power, the LT of the interference power equals

$$\mathcal{L}_I(s) = \exp\Big(-p\lambda_u\pi\frac{\Gamma\big(m+\frac{2}{\eta}\big)}{\Gamma(m)m^{\frac{2}{\eta}}}\Gamma(1-\frac{2}{\eta})s^{\frac{2}{\eta}}\Big). \tag{6}$$

Authors in [17] noted the LT in (6) follows belongs to a class of Kohlrausch-Williams-Watts (KWW) functions defined as $\mathcal{L}_I(s;\beta) = e^{-s^\beta}$, with parameter β defined as [18]

$$\mathcal{L}_I(s;\beta) = \int_0^\infty \exp(-sI) f_I(x;\beta)\mathrm{d}I = \exp(-s^\beta), \tag{7}$$

and provide closed-form expressions of the interference power PDF $f_I(x;\beta)$ for rational (fractional) values of β.

For suburban environments, we set the path loss exponent to $\eta = 4$, leading to the well-known closed-form expression for interference power PDF, also known as Lévy distribution, with scale parameter $\beta = \frac{1}{2}$

$$f_I(x) = \frac{t\exp(-\frac{t^2}{4x})}{2\sqrt{\pi}x^{\frac{3}{2}}}, \tag{8}$$

where $t = \pi p\lambda_u\frac{\Gamma\left(m+\frac{2}{\eta}\right)}{\Gamma(m)m^{\frac{2}{\eta}}}\Gamma(1-\frac{1}{2})$. However, we note that the subsequent analysis is valid for any rational value of β for which $f_I(x)$ is available in the closed form [17].

III. Error Probability at the Nearest BS

1) Asymptotic (threshold-based) Error Probability: The threshold-based decoding criteria, commonly considered in the literature, assumes that an error event occurs if the SINR γ, defined in (3), is below a predefined threshold γ_{th}. Formally, the error probability P_e (also referred to as the outage probability) can be expressed as

$$P_e = \mathbb{P}[\gamma \le \gamma_{\mathrm{th}}] = \mathbb{P}\Big[\frac{hr^{-\eta}}{I} \le \gamma_{\mathrm{th}}\Big] = 1 - \mathbb{P}[I \le \frac{hr^{-\eta}}{\gamma_{\mathrm{th}}}], \tag{9}$$

where γ_{th} represents the SINR threshold.

The probability that a device, affected by Nakagami fading, is not decoded at the nearest BS under the threshold-based criterion can be determined as

$$P_e = 1 - \int_0^\infty \left(\int_0^\infty \left(\int_0^{\frac{hr^{-\eta}}{\gamma_{\rm th}}} f_I(x)\mathrm{d}x \right) f_H(h)\mathrm{d}h \right) f_R(r)\mathrm{d}r, \quad (10)$$

where $f_H(h)$ is defined in (4). In the nearest BS model, the device attaches to the geographically nearest BS. The PDF of the distance R between the device and the nearest BS for a PPP is [10]

$$f_R(r) = 2\pi\lambda_b r \exp(-\lambda_b \pi r^2), \quad r \in (0, +\infty]. \quad (11)$$

For the suburban environment closed-form expression for the asymptotic (threshold-based) error probability is given in [14] and can be expressed as

$$P_e = 1 - \frac{1}{\Gamma(m)\pi} G_{3,3}^{3,2}\left(\frac{t^2 \gamma_{\rm th} m}{(\lambda_b \pi)^2} \,\middle|\, \begin{matrix} 0, \frac{1}{2}, 1 \\ \frac{1}{2}, m, 0 \end{matrix} \right). \quad (12)$$

where $G_{p,q}^{m,n}(\cdot\,|\,\cdot)$ is the Meijer's *G*-function [19, (9.301)]. Analysis is valid for any rational value of β for which $f_I(x)$ is available in the closed form. Note that this result is a closed-form solution, completing the approximate analysis in [10].

Approximation: After applying [19, (07.34.06.0001.01)] to transform the Meijer's *G*-function into a series form when its argument tends to zero, and after removing the higher-order terms of the series representation, the approximation of the threshold-based error probability for large values of λ_b and/or low values of λ_u or p is derived as

$$P_e \approx 3cz^{\frac{1}{2}} - (-1)^m m z^m, \quad (13)$$

where $z = \frac{t^2 \gamma_{\rm th} m}{(\lambda_b \pi)^2}$ and $c = \frac{\Gamma(m-\frac{1}{2})}{3\sqrt{\pi}\Gamma(m)}$. For the complete derivation plese refer to [14], Appendix B.

2) Finite Block-length Error Probability: We adopt a more practical model in which devices transmit short packets encoded with finite-length error-correcting codes. Using FBL information theory, for a code of length n and the target error probability ϵ, the maximal achievable code rate $R(n;\epsilon,\gamma)$ can be approximated via normal approximation [7]

$$R(n;\epsilon,\gamma) = C(\gamma) - \sqrt{\frac{V(\gamma)}{n}} Q^{-1}(\epsilon), \quad (15)$$

where $Q^{-1}(\cdot)$ denotes the inverse of $Q(x) = \int_x^\infty \frac{1}{2\pi} e^{-\frac{t^2}{2}} dt$ (the Gaussian Q-function), $V(\gamma) = \gamma \frac{\gamma+2}{(1+\gamma)^2} \log_2^2(e)$ is channel dispersion, and $C(\gamma) = \log_2(1+\gamma)$ is Shannon capacity. From (15), and treating interference as a noise, we approximate the error probability conditioned on the SINR γ as

$$\epsilon(\gamma) = Q\left(\sqrt{\frac{n}{V(\gamma)}} \big(C(\gamma) - R\big) \right). \quad (16)$$

By conditioning the error probability over γ, and further over h and r, we obtain the FBL equivalent[1] of the expression (10)

$$\begin{aligned} P_e^{\rm fbl} &= \epsilon = \int_\gamma \epsilon(\gamma) f_\Gamma(\gamma)\mathrm{d}\gamma \\ &= \int_r \left(\int_h \left(\int_\gamma \epsilon(\gamma) f_\Gamma(\gamma|h,r)\mathrm{d}\gamma \right) f_H(h)\mathrm{d}h \right) f_R(r)\mathrm{d}r, \end{aligned} \quad (17)$$

where $f_H(h)$ and $f_R(r)$ are defined in (4) and (11), respectively, and $f_\Gamma(\gamma|h,r)$ can be evaluated as

$$f_\Gamma(\gamma|h,r) = f_I(\Phi^{-1}(\gamma)) \left| \frac{\mathrm{d}\,\Phi^{-1}(\gamma)}{\mathrm{d}\gamma} \right| = \frac{t \exp(-\frac{t^2}{4\frac{hr^{-4}}{\gamma}})}{2\sqrt{\pi}\sqrt{hr^{-4}}}, \quad (18)$$

where the PDF $f_I(x)$ is given in (8). Although (17) can not be derived as a closed-form expression, it can be efficiently evaluated by numerical integration.

Approximation: In order to approximate (17), we use a linearization technique [20] for the Q-function in (16), i.e., $Q\Big(\sqrt{\frac{n}{V(\gamma)}}\big(C(\gamma) - R\big)\Big) \simeq J(\gamma)$ at point $\gamma = \theta$, to write

$$J(\gamma) = \begin{cases} 1, & \gamma \le \theta - a \\ \frac{1}{2} - \frac{\mu}{\sqrt{2\pi}}(\gamma - \theta), & \theta - a \le \gamma \le \theta + a \\ 0, & \gamma \ge \theta + a \end{cases}, \quad (19)$$

where $a = \sqrt{\frac{\pi}{2\mu^2}}$ for $\theta = 2^R - 1$, $\mu = \sqrt{\frac{n}{2\pi(2^{2R}-1)\log_2^2 e}}$. Following derivation in [14], Appendix A, the error probability in (17) is tightly approximated as

$$\begin{aligned} P_e^{\rm fbl} \approx & \frac{a_1}{\Gamma(m)\pi} G_{3,3}^{2,3}\left(z_1 \,\middle|\, \begin{matrix} 1,0,\frac{1}{2} \\ \frac{1}{2}, m, 0 \end{matrix} \right) + \frac{a_2}{\Gamma(m)\pi} G_{3,3}^{2,3}\left(z_2 \,\middle|\, \begin{matrix} 1,0,\frac{1}{2} \\ \frac{1}{2}, m, 0 \end{matrix} \right) \\ & - b_1 z_1 \big(c + d {z_1}^{m-\frac{1}{2}}\big) + b_2 z_2 \big(c + d {z_2}^{m-\frac{1}{2}}\big), \end{aligned} \quad (20)$$

where

$$\begin{aligned} a_1 &= \left(\frac{1}{2} + \frac{\mu\theta}{\sqrt{2\pi}}\right), \quad a_2 = \left(\frac{1}{2} - \frac{\mu\theta}{\sqrt{2\pi}}\right) \\ b_1 &= \frac{\mu(\theta+a)}{\sqrt{2\pi}}, \quad b_2 = \frac{\mu(\theta-a)}{\sqrt{2\pi}}, \\ z_1 &= \frac{t^2(\theta+a)m}{(\lambda_b\pi)^2}, \quad z_2 = \frac{t^2(\theta-a)m}{(\lambda_b\pi)^2}, \\ c &= \frac{\Gamma(m-\frac{1}{2})}{3\sqrt{\pi}\Gamma(m)}, \quad d = \frac{(-1)^m m}{m+1}, \end{aligned} \quad (21)$$

where $G_{p,q}^{m,n}(\cdot\,|\,\cdot)$ is the Meijer's *G*-function [16].

For practical system parameters ($\frac{t^2(\theta\pm a)m}{(\lambda_b\pi)^2} \to 0$), note that argument of the Meijer's *G*-functions in (20) is very small . Series representations of Meijer's *G*-function when its argument tends to zero can be applied by utilizing [19,

[1]Note that, by treating interference as a noise, we interpret $\gamma_{\rm th}$ in (9) as the threshold (minimal) SNR value under which the error probability of capacity-achieving error correction code of rate R vanishes as its code length n tends to infinity (justifying the term asymptotic error probability). Thus for a given R, one can calculate $\gamma_{\rm th}$ below which error probability tends to one as the code length $n \to \infty$, which is used as an SINR threshold in the asymptotic case.

(07.34.06.0001.01)], which lead to the simple closed-form expression of the error probability derived in [14]

$$P_{e,\mathrm{app}}^{\mathrm{fbl}} \approx a_1\big(3cz_1{}^{\frac{1}{2}} + (-1)^m z_1^m\big) + a_2\big(3cz_2^{\frac{1}{2}} + (-1)^m z_2^m\big) - b_1 z_1\big(c + dz_1{}^{m-\frac{1}{2}}\big) + b_2 z_2\big(c + dz_2{}^{m-\frac{1}{2}}\big). \tag{22}$$

IV. Error Probability Macro reception diversity method

We consider a more realistic scenario where a transmitted packet is received by all neighboring BS. The transmission is seen as unsuccessful if the SINR at each BS is below the capture ratio threshold. In other words, if none of the BSs receive a SINR higher than the capture ratio, the packet transmission fails. This approach is referred to as "selective combining" (SC), resembling macro reception diversity. In this section, we evaluate SC-based macro diversity within one-shot random access scenarios.

Although the cumulative interference experienced by two distinct BSs is partially correlated, since a transmitting device generates interference at multiple BSs, we reasonably assume that the interference at different BSs is independent. This assumption is supported by two factors. First, empirical studies show that the interference correlation coefficient tends to zero when BSs are in different locations, following a path-loss model of the form $r^{-\eta}$ (as discussed in [4]). Second, each interference contribution undergoes fading, which is modeled as independent and identically distributed (i.i.d.) random variables across BSs. As a result, the packet loss rate, denoted by $P_{e,m}$ (where m represents macro reception diversity), is expressed as the expectation of the product of the failure probabilities across all BSs

$$P_{e,m} = \mathbb{E}\Big[\prod_{y_i \in \Phi_b} (1 - P_s(r_{y_i}))\Big], \text{with } r_{y_i} \in [0, \infty] \tag{23}$$

where r_{y_i} represents the distance between device and corresponding BS with coordinate y_i. Formula (23) is Probability Generating Fulctional (PGFL) of PPP Φ_b for BS, where $\mathbb{E}[\prod_{x\in\Phi} f(x)] = \exp(-\lambda(\int_{\mathbb{R}^2}(1 - f(x))\mathrm{d}x))$, and thus the term in (23) can be expressed like:

$$P_{e,m} = \exp\Big\{ - 2\pi\lambda_b \int_0^\infty P_s(r) r \mathrm{d}r \Big\} \tag{24}$$

We focus on the primary task of computing the error probability associated with the decoding of an active IoT user at the macro BS. We will explore both the FBL method and the asymptotic (threshold-based) approach to address this challenge.

1) Asymptotic (threshold-based) Error Probability: In this case we will explore classical asymptotic analysis based on threshold-based error probability. In this approach, error determination relies on the comparison of the SINR, denoted as γ, against a predefined threshold, γ_{th}. We aim to derive the specific value of the SINR threshold, γ_{th}, given a certain R (rate) and as n tends to infinity, particularly focusing on the scenario involving macro BS.

Formally, the asymptotic error probability $P_{e,m}$ can be expressed as

$$P_{e,m} = \mathbb{P}[\gamma \le \gamma_{\mathrm{th}}] = \mathbb{P}\Big[\frac{hr^{-\eta}}{I} \le \gamma_{\mathrm{th}}\Big] = 1 - \mathbb{P}\Big[I \le \frac{hr^{-\eta}}{\gamma_{\mathrm{th}}}\Big], \tag{25}$$

where γ_{th} represents the SINR threshold.

The probability that a device, affected by Nakagami fading, is not decoded at the nearest BS under the threshold-based criterion can be determined as

$$P_{e,m} = \exp\Big(-2\pi\lambda_b \int_0^\infty \Big(\int_0^\infty \Big(\int_0^{\frac{hr^{-4}}{\gamma_{\mathrm{th}}}} f_I(x)\mathrm{d}x\Big) f_H(h)\mathrm{d}h\Big) r\mathrm{d}r\Big), \tag{26}$$

where PDF of fading and interference are already defined in (4) and (8) respectively, and parameter $t = \pi p \lambda_u \frac{\Gamma\left(m+\frac{2}{\eta}\right)}{\Gamma(m) m^{\frac{2}{\eta}}} \Gamma(1 - \frac{2}{\eta})$. For the suburban environment we present a novel closed-form expression for the asymptotic error probability as

$$P_{e,m} = \exp\Big(- \frac{2\lambda_b}{\pi p \lambda_u \sqrt{\gamma_{\mathrm{th}}}}\Big) \tag{27}$$

Analysis is valid for any rational value of β for which $f_I(x)$ is available in the closed form. Note that this result is a closed-form solution. Complete derivation is shown in Appendix A.

2) FBL Error Probability: Utilizing the FBL error probability definition previously provided in equation (16), we can derive the ultimate expression for the error probability in the considered uplink communication system. By conditioning the error probability from equation (16) on the interference γ, and subsequently conditioning the interference on fading h we come to the comprehensive FBL error probability expression.

$$P_{e,m}^{\mathrm{fbl}} = \int_\gamma \epsilon(\gamma) f_\Gamma(\gamma)\mathrm{d}\gamma = \exp\Big(-2\pi\lambda_b \epsilon \int_r \Big(\int_h \Big(\int_\gamma \epsilon(\gamma) f_\Gamma(\gamma|h,r)\mathrm{d}\gamma\Big) f_H(h)\mathrm{d}h\Big) f_R(r)\mathrm{d}r\Big). \tag{28}$$

In (28), $f_H(h)$ is defined in (4) and $f_R(r) = r$. Furthermore, the conditional SINR distribution $f_\Gamma(\gamma|h,r)$ can be obtained using (3), and evaluated as

$$f_\Gamma(\gamma|h,r) = f_I(\Phi^{-1}(\gamma))\left|\frac{\mathrm{d}\Phi^{-1}(\gamma)}{\mathrm{d}\gamma}\right| = \frac{t\exp(-\frac{t^2\gamma}{4hr^{-4}})}{2\sqrt{\pi h r^{-4}\gamma}}, \tag{29}$$

where the PDF $f_I(x)$ is given in (8). Although (28) can not be derived as a closed-form expression, it can be evaluated by numerical integration.

Approximation: Given that the error probability in equation (28) cannot be obtained as a closed-form expression, we resort to employing the linear approximation of the Q-function as

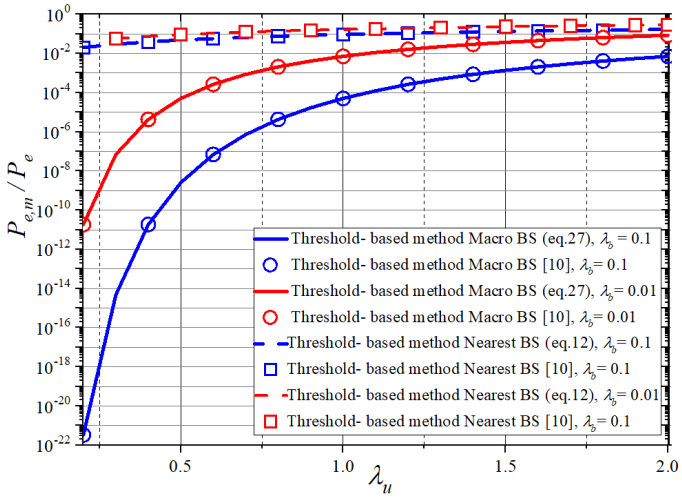

Fig. 2. Error probability $P_e, P_{e,m}$ vs. density of users λ_u for asymptotic threshold-based for nearest and macro BS methods (12) and (27). Different λ_b is used, activation rate is $p = 0.01$ and threshold is $\gamma_{\text{th}} = 0.4142$.

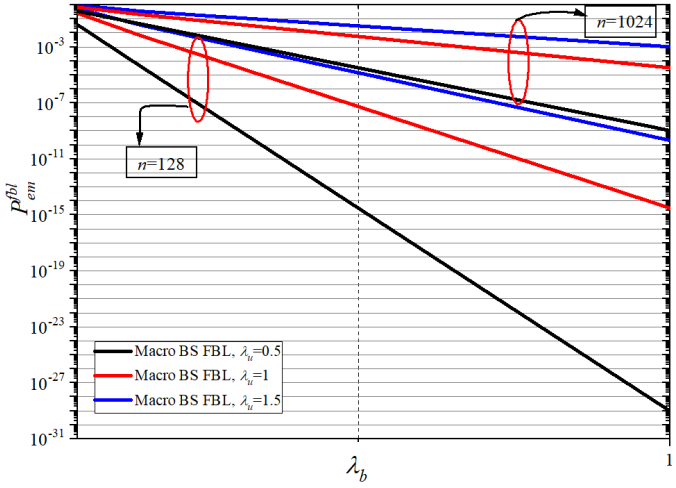

Fig. 3. Error probability vs. λ_b for macro diversity reception method in FBL regime $P^{\text{fbl}}_{e,m}$ where $m = 1$, $R = 1/2$ and $n = 128$ and $n = 1024$.

depicted in equation (19). For short-packet uplink communications, after conducting the derivation outlined in Appendix B, we can closely approximate the error probability as follows:

$$P^{\text{fbl}}_{e,m} \approx \exp\left(-\frac{2\lambda_b}{\pi p\lambda_u}a_{m1}^{-1}\right) + \exp\left(-\frac{\lambda_b}{\pi p\lambda_u}\left(a_{m2}^{-1}-a_{m1}^{-1}\right)\right.$$
$$\left.\times\frac{\sqrt{2}\lambda_b\mu}{\sqrt{\pi}p\lambda_u}\left(a_{m2}^{-1}-a_{m1}^{-1}\right) - \frac{\mu\theta}{\sqrt{\pi}}\frac{\sqrt{2}\lambda_b}{\pi p\lambda_u}\left(a_{m1}-a_{m2}\right)\right), \tag{30}$$

where $a_{m1} = \sqrt{\theta - a}$ and $a_{m2} = \sqrt{\theta + a}$.

V. Numerical Results

Fig. 2 shows the error probabilities P_e and $P_{e,m}$ a device experiences at its nearest and macro BS for two values of BS density ($\lambda_b = 0.01$ and $\lambda_b = 0.1$), under varying density of users λ_u, with a fixed device activity rate of $p = 0.01$. The results of the closed-form expression (12) and (27) match the results from [10], validating the analysis from Sec. III and IV. The graph demonstrates the following trends: i) increasing the BS density λ_b decreases the error probability due to the shift of $f(r)$ towards lower distances; ii) error probability increases with higher λ_u due to increased interference; and iii) error probability is lower for macro BS regime than for nearest BS regime, as expected. Additionally, error probability results, as derived in [10], are also presented in Fig.3, overlapping with our results.

Fig. 3 presents the error probability dependence on the BSs spatial density λ_b for macro diversity reception in FBL regime ($P^{\text{fbl}}_{e,m}$) method. We assume normal approximation achieving code of the same rate and $n = 128$ and $n = 1024$. The error probability is presented for several values of users densities λ_u. Increasing both the code length n and the density of users λ_u, the error probability deteriorates, due to the increase in aggregate interference.

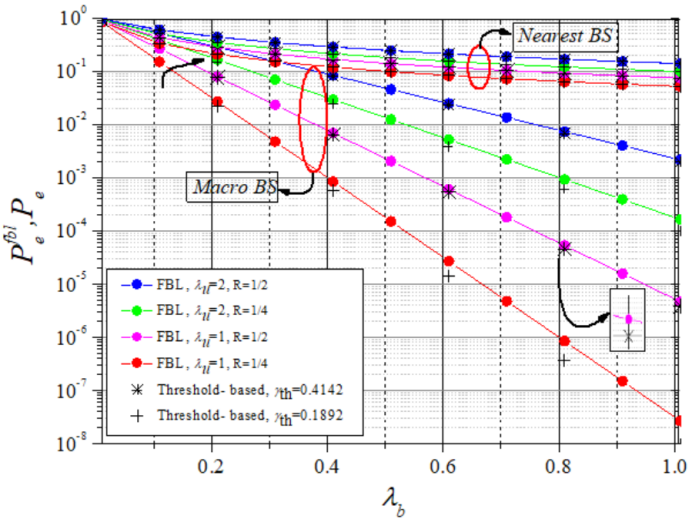

Fig. 4. Error probability vs. λ_b for asymptotic method P_e, where $\gamma_{th} = 0.4142$ and $\gamma_{th} = 0.1892$ and $n \to \infty$, and FBL method P^{fbl}_e with $R = 1/2$ and $R = 1/4$ and $n = 1024$.

Fig. 4 presents the error probability dependence on the BSs spatial density λ_b for both asymptotic (P_e) and FBL (P^{fbl}_e) method and for nearest and macro reception methods. For the former, we assume capacity-achieving error-correcting code of rate $R = \frac{1}{2}$, $R = \frac{1}{4}$ and length $n \to \infty$, while for the latter, we assume normal approximation achieving code of the same rate and $n = 1024$ (FBL). In order to mitigate transmission latency and yield high reliability, codeword lengths of the order of $n \approx 100$ symbols are most commonly used in simulation studies [3], [7]. The error probability is presented for several values of users densities λ_u. Increasing both the rate R and the density of users λ_u, the error probability deteriorates, due to the increase in aggregate interference. Macro BS model is advantageous over the nearest BS model for several reasons, primarily due to its diversity and redundancy benefits which

is depicted in the graph.

VI. Conclusion

We derived an exact expression for the error probability experienced by an LPWAN device using the nearest BS and macro diversity regime, accounting for Nakagami fading and interference from PPP distributed interferers. This model is then extended to a finite-block length scenario, where we derive an approximate error probability based on FBL information theory. A detailed derivation is provided, along with an analysis of the numerical accuracy of the exact and approximate expressions, demonstrating their application in LPWAN system design. For future work, we plan to extend these results to various fading and shadowing distributions and explore random access models beyond the widely used SA protocol.

Acknowledgment

This work has received funding from the Horizon 2020 research and innovation staff exchange grant agreement No 101086387, the 2021-2023 China-Serbia Inter- Governmental S&T Cooperation Project (No. 6), the Science Fund of the Republic of Serbia, grant number 6707, REmote WAter quality monitoRing anD IntelliGence – REWARDING and by the Secretariat for Higher Education and Scientific Research of the Autonomous Province of Vojvodina through the project "Visible light technologies for indoor sensing, localization and communication in smart buildings" (142-451-2686/2021).

Appendix A

In order to derive the threshold-based error probability in (27), the first step is to substitute the interference PDF $f_I(x)$ given by (8) in (26)

$$P_{e,m}=\exp\!\left(\!-2\pi\lambda_b\!\int_0^\infty\!\!\left(\!\int_0^\infty\!\!\left(\!\int_0^{\frac{hr^{-4}}{\gamma_{\rm th}}}\!\frac{te^{-\frac{t^2}{4x}}}{2\sqrt{\pi}x^{\frac{3}{2}}}\mathrm{d}x\!\right)\!f_H(h)\mathrm{d}h\!\right)\!r\mathrm{d}r\!\right)\!. \tag{31}$$

The inner integral over x is solved by [16, (3.361.1)] as $\int_0^{\frac{hr^{-4}}{\gamma_{\rm th}}}\frac{te^{-\frac{t^2}{4x}}}{2\sqrt{\pi}x^{\frac{3}{2}}}\mathrm{d}x = \mathrm{erfc}\!\left(\frac{t}{2}\sqrt{\frac{\gamma_{\rm th}}{hr^{-4}}}\right)$, where $\mathrm{erfc}(\cdot)$ is the complementary error function defined in [16, (8.250.4)]. After substituting solution of the integral over x in (31), and the replacement of the PDF of the fading power given by (4), the error probability in (26) is rewritten as

$$P_{e,m} = \exp\!\left(-2\pi\lambda_b\int_0^\infty\!\left(\int_0^\infty \mathrm{erfc}\!\left(\frac{t}{2}\sqrt{\frac{\gamma_{\rm th}}{hr^{-4}}}\right)\times\frac{m^m}{\Gamma(m)}h^{m-1}e^{-mh}\mathrm{d}h\right)r\mathrm{d}r\right). \tag{32}$$

Exponential function is represented in terms of Meijer's *G*-function [19, (01.03.26.0004.01)] as $e^{-h}=G_{0,1}^{1,0}\big(h\,\big|\,{-\atop 0}\big)$, while [19, (06.27.26.0006.01) and (07.34.16.0002.01)] can be used for the complementary error function as $\mathrm{erfc}\!\left(\frac{t}{2}\sqrt{\frac{\gamma_{\rm th}}{hr^{-4}}}\right) = \frac{1}{\sqrt{\pi}}G_{2,1}^{0,2}\!\left(\frac{4r^{-4}h}{t^2\gamma_{\rm th}}\,\middle|\,{1,\frac{1}{2}\atop 0}\right)$. Afterwards, the error probability in (32) can be written as

$$P_{e,m}=\exp\!\left(-2\pi\lambda_b\frac{m^m}{\sqrt{\pi}\Gamma(m)}\int_0^\infty\!\!\left(\int_0^\infty\!\!h^{m-1}G_{0,1}^{1,0}\big(mh\,\big|\,{-\atop 0}\big)\times G_{2,1}^{0,2}\!\left(\frac{4r^{-4}}{t^2\gamma_{\rm th}}h\,\middle|\,{1,\frac{1}{2}\atop 0}\right)\!dh\right)\!r\mathrm{d}r\right). \tag{33}$$

Integral over h in (33) is solved by [19, (07.34.21.0011.01)] as

$$\begin{aligned}&\int_0^\infty h^{m-1}G_{0,1}^{1,0}\big(mh\big|\,{-\atop 0}\big)G_{2,1}^{0,2}\!\left(\frac{4r^{-4}h}{t^2\gamma_{\rm th}}\,\middle|\,{1,\frac{1}{2}\atop 0}\right)\mathrm{d}h\\&=m^{-m}G_{3,1}^{0,3}\!\left(\frac{4r^{-4}}{t^2\gamma_{\rm th}m}\,\middle|\,{1,\frac{1}{2},1-m\atop 0}\right).\end{aligned} \tag{34}$$

After substituting (34) into (33), the error probability is rewritten as

$$P_{e,m}=\exp(-\frac{2\pi\lambda_b}{\Gamma(m)\sqrt{\pi}}\int_0^\infty rG_{3,1}^{0,3}\!\left(\frac{4r^{-\eta}}{t^2\gamma_{th}m}\,\middle|\,{1,\frac{1}{2},1-m\atop 0}\right)\!dr. \tag{35}$$

After applying the change of variables $r^2=u$, [19, (07.34.16.0002.01)] is used to perform transformation of Meijer's *G*-function as

$$G_{3,1}^{0,3}\!\left(\frac{4u^{-2}}{t^2\gamma_{\rm th}m}\,\middle|\,{1,\frac{1}{2},1-m\atop 0}\right)=G_{1,3}^{3,0}\!\left(\frac{t^2\gamma_{\rm th}m}{4}u^2\,\middle|\,{1,\frac{1}{2},m\atop 0,\frac{1}{2},m}\right), \tag{36}$$

Finally, the error probability expression is re-written as

$$P_{e,m}=\exp\!\left(-\frac{2\sqrt{\pi}\lambda_b}{\Gamma(m)\eta}\int_0^\infty x^{\frac{2}{\eta}-1}G_{3,1}^{0,3}\!\left(\frac{4}{t^2\gamma_{th}m}x^{-1}\,\middle|\,{1,\frac{1}{2},1-m\atop 0}\right)\!\mathrm{d}x\right). \tag{37}$$

Integral in (37) is solved with the help of [19, (07.34.21.0009.01)], and derived final closed-form expression for the threshold-based error probability is given in (27).

Appendix B

Approximation of $Q(\cdot)$ function at point $\theta=2^R-1$ based on a linearization technique was shown in (19). After substituting (19) into (17), the approximation of the error probability is defined as

$$\begin{aligned}P_{e,m}^{\rm fbl}\approx&\exp\!\left(-2\pi\lambda_b\!\left(\int_0^\infty\!\!\left(\int_0^\infty\!\!\left(\int_0^{\theta-a}\!f_\Gamma(\gamma|h,r)\mathrm{d}\gamma\right)\!f_H(h)\mathrm{d}h\right)\!r\mathrm{d}r\right)\right)\\&+\exp\!\left(-2\pi\lambda_b\!\left(\int_0^\infty\!\!\left(\int_0^\infty\!\!\left(\int_{\theta+a}^{\theta-a}\!\frac{1}{2}f_\Gamma(\gamma|h,r)\mathrm{d}\gamma\right)\!f_H(h)\mathrm{d}h\right)\!r\mathrm{d}r\right.\right.\\&-\int_0^\infty\!\!\left(\int_0^\infty\!\!\left(\int_{\theta+a}^{\theta-a}\!\frac{\mu\gamma}{\sqrt{2\pi}}f_\Gamma(\gamma|h,r)\mathrm{d}\gamma\right)\!f_H(h)\mathrm{d}h\right)\!r\mathrm{d}r\\&\left.\left.+\int_0^\infty\!\!\left(\int_0^\infty\!\!\left(\int_{\theta+a}^{\theta-a}\!(\frac{\mu\theta}{\sqrt{2\pi}}f_\Gamma(\gamma|h,r)\mathrm{d}\gamma\right)\!f_H(h)\mathrm{d}h\right)\!r\mathrm{d}r\right)\right)\\&=I_1+\exp(-2\pi\lambda_b(I_2-I_3+I_4))\end{aligned} \tag{38}$$

where μ and a are previously defined in Sec. III, and triple integrals in (38) are defined as

$$I_1 = \exp\Bigg(-2\pi\lambda_b \int_0^{\infty}\Bigg(\int_0^{\infty}\Bigg(\int_0^{\theta-a} f_{\Gamma}(\gamma|h,r)\mathrm{d}\gamma\Bigg) f_H(h)\mathrm{d}h\Bigg) r\mathrm{d}r\Bigg), \tag{39}$$

$$I_2 = \int_0^{\infty}\Bigg(\int_0^{\infty}\Bigg(\int_{\theta+a}^{\theta-a} \frac{1}{2} f_{\Gamma}(\gamma|h,r)\mathrm{d}\gamma\Bigg) f_H(h)\mathrm{d}h\Bigg) r\mathrm{d}r, \tag{40}$$

$$I_3 = \int_0^{\infty}\Bigg(\int_0^{\infty}\Bigg(\int_{\theta+a}^{\theta-a} \frac{\mu\gamma}{\sqrt{2\pi}} f_{\Gamma}(\gamma|h,r)\mathrm{d}\gamma\Bigg) f_H(h)\mathrm{d}h\Bigg) r\mathrm{d}r, \tag{41}$$

$$I_4 = \int_0^{\infty}\Bigg(\int_0^{\infty}\Bigg(\int_{\theta+a}^{\theta-a} \frac{\mu\theta}{\sqrt{2\pi}} f_{\Gamma}(\gamma|h,r)\mathrm{d}\gamma\Bigg) f_H(h)\mathrm{d}h\Bigg) r\mathrm{d}r. \tag{42}$$

After substituting (4) and (18) into (39), the first triple integral in (39) is re-written as

$$I_1 = \exp\Bigg(-2\pi\lambda_b \int_0^{\infty}\Bigg(\int_0^{\infty}\Bigg(\int_0^{\theta-a} \frac{te^{-\frac{t^2\gamma}{4hr^{-4}}}}{2\sqrt{\pi hr^{-4}}}\gamma^{-\frac{1}{2}}\mathrm{d}\gamma\Bigg) \times \frac{m^m}{\Gamma(m)} h^{m-1}e^{-mh}\mathrm{d}h\Bigg) r\mathrm{d}r\Bigg). \tag{43}$$

After solving the inner integral in (43) over γ with the help of [16, (8.251)] as $\int_0^{\theta-a} \frac{te^{-\frac{t^2\gamma}{4hr^{-4}}}}{2\sqrt{\pi hr^{-4}}}\gamma^{-\frac{1}{2}}\mathrm{d}\gamma = \mathrm{erf}(\frac{t\sqrt{\theta-a}}{2\sqrt{hr^{-4}}})$, the integral I_1 is now rewritten as

$$I_1 = \exp\Bigg(-\frac{2\pi\lambda_b m^m}{\Gamma(m)} \int_0^{\infty}\Bigg(\int_0^{\infty} h^{m-1}e^{-mh}\mathrm{erf}\Bigg(\frac{t\sqrt{\theta-a}}{2\sqrt{hr^{-4}}}\Bigg)\mathrm{d}h\Bigg) r\mathrm{d}r\Bigg). \tag{44}$$

After representing the exponential function in terms of Meijer's *G*-functions by using [19, (01.03.26.0004.01)] as $e^{-mh} = G_{0,1}^{1,0}\big(mh \,\big|\, \begin{smallmatrix} - \\ 0 \end{smallmatrix}\big)$, and the error function function by using [19, (06.25.26.0006.01) and (07.34.21.0011.01)] as $\mathrm{erf}(\frac{t\sqrt{\theta-a}}{2\sqrt{hr^{-4}}}) = \frac{1}{\sqrt{\pi}} G_{2,1}^{1,1}\Big(\frac{4hr^{-4}}{t^2(\theta-a)} \,\Big|\, \begin{smallmatrix} \frac{1}{2}, 1 \\ 0 \end{smallmatrix}\Big)$, respectively, the inner integral over h is solved with the help of [19, (07.34.21.0011.01)]. Afterwards, the error probability in (44) can be written as

$$I_1 = \exp\Bigg(-\frac{2\sqrt{\pi}\lambda_b}{\Gamma(m)} \int_0^{\infty} r G_{3,1}^{1,2}\Bigg(\frac{4r^{-4}}{t^2(\theta-a)m} \,\Bigg|\, \begin{smallmatrix} \frac{1}{2}, 1-m, 1 \\ 0 \end{smallmatrix}\Bigg)\mathrm{d}r\Bigg). \tag{45}$$

Applying the change of variables $r^{\eta} = x$, (45) is re-written as , the integral I_1 is finally solved with the help of [19, (07.34.16.0002.01) and (07.34.21.0009.01)] as

$$\begin{aligned} I_1 &= \exp\Bigg(-\frac{2\sqrt{\pi}\lambda_b}{\Gamma(m)\eta}\Bigg(\int_0^{\infty} x^{\frac{2}{\eta}-1} G_{1,3}^{2,1}\Bigg(\frac{t^2(\theta-a)mx}{4} \,\Bigg|\, \begin{smallmatrix} 1 \\ \frac{1}{2}, m, 0 \end{smallmatrix}\Bigg)\mathrm{d}x\Bigg) \\ &= \exp\Bigg(-\frac{2\lambda_b}{\pi p\lambda_u}\frac{1}{\sqrt{\theta-a}}\Bigg). \end{aligned} \tag{46}$$

Next, we will deal with the second triple integral I_2 in (40). After substituting (4), and (18) into (40), the integral I_2 is re-written as

$$I_{21} = \int_0^{\infty}\Bigg(\int_0^{\infty}\Bigg(\int_{\theta-a}^{\theta+a} \frac{te^{-\frac{t^2\gamma}{4hr^{-4}}}}{4\sqrt{\pi hr^{-4}}}\gamma^{-\frac{1}{2}}\mathrm{d}\gamma\Bigg) \times \frac{m^m}{\Gamma(m)} h^{m-1}e^{-mh}\mathrm{d}h\Bigg) r\mathrm{d}r, \tag{47}$$

The inner integral in (47) over γ is solved by [16, (8.251)] as $\int_{\theta-a}^{\theta+a} \frac{te^{-\frac{t^2\gamma}{4hr^{-4}}}}{4\sqrt{\pi hr^{-4}}}\gamma^{-\frac{1}{2}}\mathrm{d}\gamma = \frac{1}{2}\,\mathrm{erf}(\frac{t\sqrt{\theta+a}}{2\sqrt{hr^{-4}}}) - \frac{1}{2}\,\mathrm{erf}(\frac{t\sqrt{\theta-a}}{2\sqrt{hr^{-4}}})$, leading to the new form of integral I_{21}

$$I_2 = \int_0^{\infty}\Bigg(\int_0^{\infty}\Bigg(\frac{1}{2}\,\mathrm{erf}(\frac{t\sqrt{\theta+a}}{2\sqrt{hr^{-4}}}) - \frac{1}{2}\,\mathrm{erf}(\frac{t\sqrt{\theta-a}}{2\sqrt{hr^{-4}}})\Bigg) \times \frac{m^m}{\Gamma(m)} h^{m-1}e^{-mh}\mathrm{d}h\Bigg) r\mathrm{d}r. \tag{48}$$

Since both integrals over h and r in (48) are similar as the corresponding ones in (44), after following the same steps early described (derivation from (44) to (46)), the final expression of I_{21} is determined as

$$I_2 = \frac{1}{2\pi^2 p\lambda_u}\Bigg(\frac{1}{\sqrt{\theta+a}} - \frac{1}{\sqrt{\theta-a}}\Bigg). \tag{49}$$

After substituting (4), and (18) into (42), integral I_4 is re-written and solved by following the same procedure as in derivation of I_2

$$\begin{aligned} I_4 &= \int_0^{\infty}\Bigg(\int_0^{\infty}\Bigg(\int_{\theta-a}^{\theta+a} \frac{\mu\theta}{\sqrt{2\pi}}\frac{te^{-\frac{t^2\gamma}{4hr^{-4}}}}{2\sqrt{\pi hr^{-4}}}\gamma^{-\frac{1}{2}}\mathrm{d}\gamma\Bigg) \times \frac{m^m}{\Gamma(m)} h^{m-1}e^{-mh}\mathrm{d}h\Bigg) r\mathrm{d}r \\ &= \frac{\mu\theta}{\sqrt{2\pi}}\frac{1}{\pi^2 p\lambda_u}\Bigg(\frac{1}{\sqrt{\theta+a}} - \frac{1}{\sqrt{\theta-a}}\Bigg). \end{aligned} \tag{50}$$

After substituting (4), and (18) into (41), the integral I_3 is re-written as

$$I_3 = \int_0^{\infty}\Bigg(\int_0^{\infty}\Bigg(\int_{\theta-a}^{\theta+a} \frac{\mu te^{-\frac{t^2\gamma}{4hr^{-4}}}}{2\pi\sqrt{2hr^{-4}}}\gamma^{\frac{1}{2}}\mathrm{d}\gamma\Bigg) \times \frac{m^m}{\Gamma(m)} h^{m-1}e^{-mh}\mathrm{d}h\Bigg) r\mathrm{d}r, \tag{51}$$

The inner integral in (51) over γ is solved as

$$\begin{aligned} I_3 = \int_0^{\infty}\Bigg(\int_0^{\infty} \frac{\mu t}{2\pi\sqrt{2hr^{-\eta}}}\frac{m^m}{\Gamma(m)} h^{m-1}e^{-mh}\mathrm{d}h\Bigg) \\ \times \Bigg((\theta+a)^{\frac{3}{2}} E_{-\frac{1}{2}}\big(\frac{t^2}{4hr^{-\eta}}(\theta+a)\big) \\ - (\theta-a)^{\frac{3}{2}} E_{-\frac{1}{2}}\big(\frac{t^2}{4hr^{-\eta}}(\theta-a)\big)\Bigg) r\mathrm{d}r, \end{aligned} \tag{52}$$

where $E_v(z)$ represents exponential integral defined in [19, (06.34.07.0001.01)]. Exponential function is represented in terms of Meijer's *G*-function by [19, (01.03.26.0004.01)] as $e^{-h} = G_{0,1}^{1,0}\big(h \,\big|\, \begin{smallmatrix} - \\ 0 \end{smallmatrix}\big)$, while [19, (06.34.26.0005.01) and (07.34.16.0002.01)] can be used to transform exponential integral function into Meijer's *G*-function. Integral over h

in (52) can be solved using [19, (07.34.21.0011.01) and (07.34.16.0002.01)] as

$$\begin{aligned} I_3 &= \frac{\mu t\sqrt{m}}{2\sqrt{2}\pi\Gamma(m)} \int_0^\infty \\ &\times \left((\theta+a)^{\frac{3}{2}} G_{1,3}^{3,0}\left(\frac{t^2(\theta+a)mr^4}{4} \,\middle|\, \begin{matrix} -\frac{1}{2} \\ -\frac{3}{2},0,m-\frac{1}{2} \end{matrix} \right) \right. \\ &\left. - (\theta-a)^{\frac{3}{2}} G_{1,3}^{3,0}\left(\frac{t^2(\theta-a)mr^4}{4} \,\middle|\, \begin{matrix} -\frac{1}{2} \\ -\frac{3}{2},0,m-\frac{1}{2} \end{matrix} \right) \right) r\mathrm{d}r \\ &= -\frac{\mu}{\sqrt{2}\pi^{\frac{3}{2}} p\lambda_u} \left(\sqrt{\theta-a} - \sqrt{\theta+a} \right). \end{aligned} \tag{53}$$

After substituting (39), (40), (41) and (42), the final approximate FBL error probability is derived and given by (30). The deviation from the exact values of error probability will be determined based on the expression given in (26), which will be calculated by numerical integration.

REFERENCES

[1] U. Raza, P. Kulkarni, and M. Sooriyabandara, "Low power wide area networks: an overview," *IEEE Commun. Surv. Tutor.,* vol. 19, no. 2, pp. 855-873, Secondquarter 2017.

[2] A. Laya, L. Alonso, and J. Alonso-Zarate, "Is the random access channel of LTE and LTE-A suitable for M2M communications? A survey of alternatives," *IEEE Commun. Surv. Tutor.*, vol. 16, no. 1, pp. 4-16, First Quarter 2014.

[3] G. Durisi, T. Koch, and P. Popovski, "Toward massive, ultrareliable, and low-latency wireless communication with short packets," *Proc. IEEE*, vol. 104, no. 9, pp. 1711-1726, Sept. 2016.

[4] M. Haenggi and R. K. Ganti, "Interference in large wireless networks," *Found. Trends Netw.*, vol. 3, no. 2, pp. 127-248, 2009.

[5] M. Haenggi, "Stochastic geometry for wireless networks," *Cambridge University Press*, 2012.

[6] F. Baccelli, B. Blaszczyszyn, and P. Muhlethaler, "An Aloha protocol for multihop mobile wireless networks," *IEEE Trans. Inf. Theory*, vol. 52, no. 2, pp. 421-436, Feb. 2006.

[7] Y. Polyanskiy, V. H. Poor, and S. Verdú, "Channel coding rate in the finite blocklength regime," *IEEE Trans. Inf. Theory*, vol. 56, no. 5, pp. 2307–2359, 2010.

[8] G. Durisi, T. Koch, J. Oestman, J. Polyanskiy, and W. Yang, "Short-packet communications over multiple-antenna Rayleigh-fading channels", *IEEE Trans. Inf. Theory*, vol. 56, no. 5, pp. 2307-2359, May 2010.

[9] T. D. Novlan, H. S. Dhillon, and J. G. Andrews, "Analytical modeling of uplink cellular networks," *IEEE Trans. Wirel. Commun,* vol. 12, no. 6, pp. 2669-2679, June 2013.

[10] Q. Song, X. Lagrange, and L. Nuaymi, "Evaluation of macro diversity gain in long range ALOHA networks," *IEEE Commun. Lett.*, vol. 21, no. 11, pp. 2472-2475, Nov. 2017.

[11] N. Hesham and A. Chaaban, "On the performance of large-scale wireless networks in the finite block-length regime," in *Proc. IEEE ICC*, Montreal, QC, Canada, pp. 1-6, 2021.

[12] N. Hesham, J. Hossain, and A. Chaaban, "Transmission rate analysis for large scale uplink networks in the finite block-length regime," in *Proc. IEEE WCNC* 2023, Glasgow, United Kingdom, pp. 1-6, 2023.

[13] T. Devaja, "Design and analysis of massive IoT networks in finite block-length regime," University of Novi Sad, 2024.

[14] T. Devaja, M. Petkovic, C. Wang, M. Beko and D. Vukobratovic, "On Error Probability Analysis of Short-Packet Communications in Massive Internet of Things," *IEEE Access*, vol. 12, pp. 67107-67116, 2024.

[15] R. Vaze, "Random Wireless Networks: An Information Theoretic Perspective," *Cambridge University Press*, 2015.

[16] I. Gradshteyn and I. Ryzhik, *Table of integrals, series, and products*, 5th ed. San Diego, CA, USA: Academic, 1994.

[17] H. A. Ammar, Y. Nasser, and H. Artail, "Closed form expressions for the probability density function of the interference power in PPP networks," in *Proc. IEEE ICC*, Kansas City, MO, USA, pp. 1-6, 2018.

[18] R. S. Anderssen, S. A. Husain, and R. J. Loy, "The Kohlrausch function: properties and applications," *Anziam J.*, vol. 45, pp.800–816, 2004.

[19] The Wolfarm Functions Site, 2008. [Online]. Available: http:/functions.wolfarm.com

[20] B. Makki, T. Svensson, and M. Zorzi, "Finite block-length analysis of spectrum sharing networks: interference-constrained scenario," *IEEE Wirel. Commun.*, vol. 4, no.4, pp. 433-436, 2015.